Robust Resource Allocation for Secure Multiple Active RIS-Aided Full Duplex Communications

Sandeep Singh[†], Arnav Mukhopadhyay[†], Raviteja Allu[‡], Keshav Singh[†], and Sandeep Kumar Singh[§]
[†]Institute of Communications Engineering, National Sun Yat-sen University, Kaohsiung, Taiwan
[‡]CONNECT, Trinity College Dublin, Dublin 2, Ireland
[§]Department of ECE, Motilal Nehru National Institute of Technology Allahabad, India
E-mail: d133070004@student.nsysu.edu.tw, gudduarnav@gmail.com, alluraviteja202@gmail.com, keshav.singh@mail.nsysu.edu.tw, sksingh@mnnit.ac.in

***Abstract*—In this work, we investigate the performance of a multi active reconfigurable intelligent surface (ARIS)-aided full duplex (FD) secure network with an imperfect channel state information (iCSI) in the presence of an eavesdropper (Eve). We aim to minimize the total power while ensuring the desired quality of service (QoS) of uplink and downlink users within available resource constraints considering the norm-bounded iCSI at each receiving node. To tackle the non-convex nature of the formulated problem, we propose an alternating optimization (AO) based algorithm that jointly optimizes the combining vector and transmit beamforming at Alice, power allocation at each uplink user, and active beamforming at ARIS. The efficacy and convergence of the proposed algorithm are validated via extensive numerical simulation. The potential of ARISs, compared to its passive RIS (PRIS) counterpart, towards a robust FD secure system is demonstrated. Finally, we discuss the impact of key parameters such as maximum amplification factor, and RIS, and CSI error on the performance of the considered system.**

***Index Terms*—Active reconfigurable intelligent surface (RIS), power minimization, full duplex (FD), beamforming design, imperfect channel state information (CSI).**

I. Introduction

The evolution of sixth-generation (6G) wireless networks has led to an exponential increase in the number of connected wireless devices and a dramatic growth in the network's capacity [1]. However, this expansion increases the risk of information leakage to unwanted eavesdroppers (Eve), as the wireless channels are inherently broadcast. This vulnerability makes users susceptible to eavesdropping attacks, posing a significant security threat as sensitive data could be exposed [2], [3]. Therefore, considering the requirements of secure communication in 6G networks, the use of reconfigurable intelligent surface (RIS) has been well motivated as one of the possible approaches to enhance the secrecy performance of such networks [4], [5].

As discussed above, the use of RIS is very impactful in secure communication; however, double fading significantly limits its performance [6]. Thus, with an aim to tackle this limitation, the concept of active RIS (ARIS) has been set forward [7], [8]. The ARISs use an additional amplifier connected to each reflecting element, allowing it to simultaneously amplify (unlike passive RIS (PRIS)) and modify the phase (similar to PRIS) of the signal at the expense of using a bit additional power [9]. This mechanism provides significant improvement in the strength of the received signal and significantly reduces the impact of double fading [7]. Therefore, considering the impact of ARIS, its usefulness in improving the secrecy performance of wireless networks was studied in [10], [11]. It is worth mentioning that the aforementioned works in [10], [11] have presented some initial studies on the impact of the ARIS in the secrecy enhancement for wireless networks. However, in practical scenarios, obtaining perfect channel state information (pCSI) for all channel links is exceedingly difficult, and uncertainties may arise in the estimated CSI [12], [13]. In addition to this, as mentioned earlier, the use of ARIS leads to a bit increase in power consumption and thus requires an optimal power allocation to ensure green communication [14]. Nevertheless, to the best of the author's knowledge, none of the existing literature explores the utility of ARIS for achieving green, robust and secure multi-user full duplex (FD) communications with imperfect cascaded channels. Besides, due to the strategic difference between uplink and downlink transmission, the design framework presented in [15] may not be efficient enough for the robust transmission design for enhanced secrecy in multi-user FD communication.

Therefore, with an aim to provide a more sophisticated and consolidated framework towards the green and robust transmission design, we investigate the performance of an multi-ARIS-aided FD system in the presence of an Eve under the influence of imperfect channel state information (iCSI). Accordingly, considering the norm-bounded iCSI at all channels, we formulate a power minimization problem that ensures the desired quality-of-service (QoS) within available resource constraints. To tackle the non-convex nature of the formulated problem, we propose an alternating optimization (AO)-based algorithm that jointly optimizes the combining vector and transmit beamforming at Alice, beamforming at the ARISs, and power allocation at each uplink user using optimization tools such as the convex upper bound approximation, and Semidefinite programming (SDP). The efficacy and convergence of the proposed algorithm are validated via extensive numerical simulations. We discuss the impact of critical parameters such as minimum power budget at each uplink user, Alice, and ARIS, and error-bound on the secrecy performance of the considered

This work was supported in part by the National Science and Technology Council of Taiwan under Grant 113-2218-E-110-009 and also in part by the Sixth Generation Communication and Sensing Research Center funded by the Higher Education SPROUT Project, the Ministry of Education of Taiwan.

979-8-3315-6946-4/25/$31.00 ©2025 IEEE

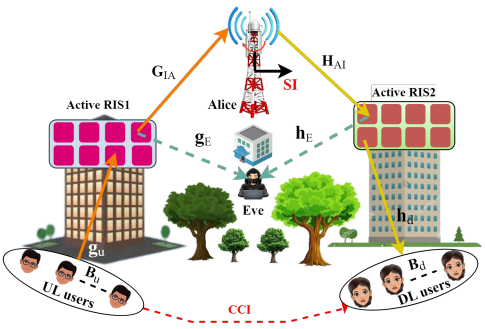

Fig. 1: System model.

system. Specifically, it is shown that ARIS can significantly reduce the required total transmission power when compared to PRIS while satisfying given QoS.

Notations: Re$(\cdot)$ represents the real component. $||\cdot||$, $||\cdot||_F$, Tr$(\cdot)$ $(\cdot)^T, (\cdot)^*$, $(\cdot)^{(n)}$ and $(\cdot)^H$ represent the Euclidean norm, F-norm, trace, transpose, conjugate, initial value, and Hermitian conjugate, respectively, of the respective matrix/vector. $\lambda_{max}(\cdot)$ and $\mathbf{u}_{max}(\cdot)$ denote the biggest eigenvalue and the associated eigenvector. diag$(\cdot)$ represents the diagonal matrix of the respective vector. $\otimes$ denotes the Kronecker product.

II. System Model

We consider a FD communication system, as illustrated in Fig. 1, consisting of an Alice serving U uplink $\{B_u^{\text{UL}}\}$ and D downlink users $\{B_d^{\text{DL}}\}$, where $u \in \mathcal{U} \triangleq \{1,\ldots,U\}$, $d \in \mathcal{D} \triangleq \{1,\ldots,D\}$. Additionally, due to unavoidable blockages, two ARISs (ARIS1 and ARIS2, one for each link) are used to provide uninterrupted communication between the devices. Moreover, the Eve tries to gather the information of the both the links and evade the secrecy aspect of the system. The Alice is equipped with M_t transmit and M_r receive antennas while all other devices (each B_u^{UL}, B_d^{DL}, and Eve) are equipped with a single antenna. In this model, the ARIS1 and ARIS2 are equipped with N and K elements, respectively, each having a power amplifier and phase shift module.

Let $\mathbf{g}_u \in \mathbb{C}^{1\times K}$, $\mathbf{h}_d \in \mathbb{C}^{1\times N}$, $\mathbf{G}_{IA} \in \mathbb{C}^{M_r\times K}$, $\mathbf{H}_{AI} \in \mathbb{C}^{N\times M_t}$, $\mathbf{g}_E \in \mathbb{C}^{1\times K}$, and $\mathbf{h}_E \in \mathbb{C}^{1\times N}$ represent the channel for the links B_u^{UL} - ARIS1, ARIS2 - B_d^{DL}, ARIS1 - Alice, Alice - ARIS2, ARIS1 - Eve, and ARIS2 - Eve, respectively, as shown in Fig. 1. Additionally, $\mathbf{\Theta}$ = diag$(\theta_1,\cdots,\theta_K) \in \mathbb{C}^{K\times K}$, and $\mathbf{\Phi}$ = diag$(\phi_1,\cdots,\phi_N) \in \mathbb{C}^{N\times N}$ denotes the diagonal matrix at active ARIS1 with $\theta_i = \eta_i e^{j\vartheta_i}$ and ARIS2 $\phi_r = \eta_r e^{j\varphi_r}$, where $\eta_i = |\mathbf{\Theta}_{[i,i]}|$, $\eta_r = |\mathbf{\Phi}_{[r,r]}|$, ϑ_i = arg$(\mathbf{\Theta}_{[i,i]}) \in [0,2\pi]$ and φ_r = arg$(\mathbf{\Phi}_{[i,i]}) \in [0,2\pi]$ are the amplification factor and phase shift at the i^{th} reflecting elements of ARIS1 and r^{th} reflecting elements of ARIS2. Note that each B_u^{UL} simultaneously transmits its respective symbol x_u and the corresponding combined signal received at Alice is given by

$$\mathbf{y}^A = \sum_{u=1}^{U} \sqrt{P_u}\mathbf{G}_{IA}\mathbf{\Theta}\mathbf{g}_u^T x_u + \mathbf{G}_{IA}\mathbf{\Theta}\mathbf{n}_I + \sqrt{\rho}\sum_{d=1}^{D}\mathbf{H}_s\mathbf{x}_d + \mathbf{n}_1, \quad (1)$$

where P_u is the transmit power used by B_u^{UL}, $\mathbf{H}_s \sim \mathcal{CN}(0,1)$ is the self-inteference (SI) channel gain, $\mathbf{x}_d$ is the signal transmit symbol from Alice to B_d^{DL}, ρ is the residual SI factor, $\mathbf{n}_I \sim \mathcal{CN}(0,\sigma_I^2\mathbf{I})$ denotes the external noise generated by the ARIS while amplifying the signals, $\mathbf{n}_1 \sim \mathcal{CN}(0,\sigma_1^2\mathbf{I})$ depict the additive white Gaussian noise (AWGN) at the Alice, respectively. Further, let $\mathbf{w}_u \in \mathbb{C}^{M_r\times U}$ represent the combining vector corresponding to B_u^{UL} and $\mathbf{W} \triangleq [\mathbf{w}_1,\cdots,\mathbf{w}_u,\cdots,\mathbf{w}_U] \in \mathbb{C}^{M_r\times U}$ represent the decoding matrix at Alice. Thus, we have

$$y_u^{\mathbf{w}} = \mathbf{w}_u^H\mathbf{G}_{IA}\mathbf{\Theta}\mathbf{g}_u^T x_u + \sum_{i=1,i\neq u}^{U}\mathbf{w}_u^H\mathbf{G}_{IA}\mathbf{\Theta}\mathbf{g}_i^T x_i + \mathbf{w}_u^H\mathbf{G}_{IA}\mathbf{\Theta}\mathbf{n}_I + \sqrt{\rho}\mathbf{w}_u^H\sum_{d=1}^{D}\mathbf{H}_s\mathbf{x}_d + \mathbf{w}_u^H\mathbf{n}_1. \quad (2)$$

Denoting $\mathbf{G}_u = \mathbf{G}_{IA}$diag$(\mathbf{g}_u^T)$ the cascaded channel from B_u^{UL} to Alice via the ARIS1 and $\boldsymbol{\theta} = [\theta_1,...,\theta_K] \in \mathbb{C}^{K\times 1}$, the signal-to-interference-plus-noise-ratio (SINR) corresponding to (2) is obtained as

$$\Upsilon_u^{\text{A}} = \frac{P_u|\mathbf{w}_u^H(\mathbf{G}_u\boldsymbol{\theta})|^2}{\Gamma_u^{\text{I}} + ||\mathbf{w}_u^H\mathbf{G}_{IA}\mathbf{\Theta}||^2\sigma_I^2 + P_u^{\text{SI}} + ||\mathbf{w}_u||^2\sigma_1^2}, \quad (3)$$

where $P_u^{\text{SI}} = \rho\sum_{d=1}^{D}|\mathbf{w}_u^H\mathbf{H}_s\mathbf{v}_d|^2$ and $\Gamma_u^{\text{I}} = \sum_{i=1,i\neq u}^{U}P_i|\mathbf{w}_u^H(\mathbf{G}_i\boldsymbol{\theta})|^2$. On a similar note, the signal received at the B_d^{DL} from the Alice can be expressed as

$$y_d = \mathbf{h}_d\mathbf{\Phi}\mathbf{H}_{AI}\mathbf{x}_d + \sum_{i=1,i\neq d}^{D}\mathbf{h}_d\mathbf{\Phi}\mathbf{H}_{AI}\mathbf{x}_i + \mathbf{h}_d\mathbf{\Phi}\mathbf{n}_I + \sum_{u=1}^{U}\sqrt{P_u}l_{u,d}x_u + n_d, \quad (4)$$

where $l_u \in \mathbb{C}^{1\times 1}$ represents the co-channel interference (CCI) link between B_u^{UL} and B_d^{DL} and $n_d \sim \mathcal{CN}(0,\sigma_d^2\mathbf{I})$ is the AWGN at B_d^{DL}. Denoting $\mathbf{H}_d$ = diag$(\mathbf{h}_d)\mathbf{H}_{AI}$ the cascaded channel from the Alice to B_d^{DL} via the ARIS2 and $\boldsymbol{\phi} = [\phi_1,...,\phi_N]^T \in \mathbb{C}^{N\times 1}$, the SINR corresponding to (4) is obtained as

$$\Upsilon_d^{\text{D}} = \frac{|(\boldsymbol{\phi}^H\mathbf{H}_d)\mathbf{v}_d|^2}{\Gamma_d^{\text{I}} + |\mathbf{h}_d\mathbf{\Phi}|^2\sigma_I^2 + P_d^{\text{CCI}} + \sigma_d^2}, \quad (5)$$

where $\mathbf{v}_d \in \mathbb{C}^{M_t\times 1}$ be the beamforming vector for B_d^{DL}, $\Gamma_d^{\text{I}} = \sum_{i=1,i\neq d}^{D}|(\boldsymbol{\phi}^H\mathbf{H}_d)\mathbf{v}_i|^2$ and $P_d^{\text{CCI}} = \sum_{u=1}^{U}P_u|l_{u,d}|^2$. The received signal at the Eve due to uplink (UL) and downlink (DL) transmission is written as

$$y^{\text{E}} = \sum_{u=1}^{U}\mathbf{g}_E\mathbf{\Theta}\mathbf{g}_u^T x_u + \mathbf{g}_E\mathbf{\Theta}\mathbf{n}_I + \sum_{d=1}^{D}\mathbf{h}_E\mathbf{\Phi}\mathbf{H}_{AI}\mathbf{x}_d + \mathbf{h}_E\mathbf{\Phi}\mathbf{n}_I + n_E, \quad (6)$$

where $n_E \sim \mathcal{CN}(0,\sigma_E^2)$ denote AWGN. The SINR corresponding to (6) are written as

$$\Upsilon_u^{\text{E}} = \frac{P_u|\mathbf{b}_u^{\text{E},H}\boldsymbol{\theta}|^2}{\Lambda_u^{\text{IE}} + |\mathbf{g}_E\mathbf{\Theta}|^2\sigma_I^2 + \Lambda^{\text{DL}} + \sigma_E^2}, \quad (7)$$

$$\Upsilon_d^{\text{E}} = \frac{|(\boldsymbol{\phi}^H\mathbf{L}_d^{\text{E}})\mathbf{v}_d|^2}{\Lambda_d^{\text{IE}} + |\mathbf{h}_E\mathbf{\Phi}|^2\sigma_I^2 + \Lambda^{\text{UL}} + \sigma_E^2}, \quad (8)$$

where $\mathbf{b}_u^{\text{E}} = \text{diag}(\mathbf{g}_E)\mathbf{g}_u^T$, $\mathbf{L}_d^{\text{E}} = \text{diag}(\mathbf{h}_E)\mathbf{H}_{AI}$, $\Lambda_u^{\text{IE}} = \sum_{i=1,i\neq u}^{U}P_i|\mathbf{b}_i^{\text{E},H}\boldsymbol{\theta}|^2$, $\Lambda_d^{\text{IE}} = \sum_{i=1,i\neq d}^{D}|(\boldsymbol{\phi}^H\mathbf{L}_d^{\text{E}})\mathbf{v}_i|^2$, $\Lambda^{\text{UL}} = \sum_{u=1}^{U}P_u|\mathbf{b}_u^{\text{E},H}\boldsymbol{\theta}|^2 + ||\mathbf{g}_E\mathbf{\Theta}||^2\sigma_I^2$, and $\Lambda^{\text{DL}} = \sum_{d=1}^{\text{D}}|(\boldsymbol{\phi}^H\mathbf{L}_d^{\text{E}})\mathbf{v}_d|^2 + ||\mathbf{h}_E\mathbf{\Phi}||^2\sigma_I^2$. The Eve possesses the capability to intercept any signal in both UL and DL transmissions, the total secrecy rate is represented as

$$R^{sec}=\Big[\sum\nolimits_{u=1}^{U}(R_u^A-R_u^{\mathrm{E}})^+ + \sum\nolimits_{d=1}^{D}(R_d^D-R_d^{\mathrm{E}})^+\Big], \quad (9)$$

where $R_i^j = \log_2(1+\Upsilon_i^j)$, $i \in \{u,d\}$, $j \in$ {A,D,E}, $[x]^+ = \max\{x,0\}$. Next, we introduce the framework of the uncertainties in the cascaded channel ($\mathbf{G}_u, \mathbf{H}_d, \mathbf{b}_u^{\mathrm{E}}$, and $\mathbf{L}_d^{\mathrm{E}}$) then the respective CSI error models. Following the concept in [12], we have $\mathbf{G}_u = \tilde{\mathbf{G}}_u + \Delta\mathbf{G}_u, \forall u \in \mathcal{U}; \mathbf{g}_u = \tilde{\mathbf{g}}_u + \Delta\mathbf{g}_u, \forall u \in \mathcal{U}; \mathbf{G}_{IA} = \tilde{\mathbf{G}}_{IA} + \Delta\mathbf{G}_{IA}; \mathbf{H}_d = \tilde{\mathbf{H}}_d + \Delta\mathbf{H}_d, \forall d \in \mathcal{D}; \mathbf{h}_d = \tilde{\mathbf{h}}_d + \Delta\mathbf{h}_d, \forall d \in \mathcal{D}; \mathbf{H}_{AI} = \tilde{\mathbf{H}}_{AI} + \Delta\mathbf{H}_{AI}; \mathbf{b}_u^{\mathrm{E}} = \tilde{\mathbf{b}}_u^{\mathrm{E}} + \Delta\mathbf{b}_u^{\mathrm{E}}, \forall u \in \mathcal{U}; \mathbf{g}_E = \tilde{\mathbf{g}}_E + \Delta\mathbf{g}_E; \mathbf{L}_d^{\mathrm{E}} = \tilde{\mathbf{L}}_d^{\mathrm{E}} + \Delta\mathbf{L}_d^{\mathrm{E}}, \forall d \in \mathcal{D}; \mathbf{h}_E = \tilde{\mathbf{h}}_E + \Delta\mathbf{h}_E$, where $(\cdot)$ is the estimated cascaded CSI and $\Delta(\cdot)$ is the respective error. Additionally, we adopt the bounded CSI error model [12], $||\Delta\mathbf{G}_u|| \le \epsilon_u, \forall u \in \mathcal{U}; ||\Delta\mathbf{g}_u|| \le \epsilon_u, \forall u \in \mathcal{U}; ||\Delta\mathbf{G}_{IA}|| \le \epsilon_u; ||\Delta\mathbf{H}_d|| \le \epsilon_d, \forall d \in \mathcal{D}; ||\Delta\mathbf{h}_d|| \le \epsilon_d, \forall d \in \mathcal{D}; ||\Delta\mathbf{H}_{AI}|| \le \epsilon_d; ||\Delta\mathbf{b}_u^{\mathrm{E}}|| \le \epsilon_E \forall u \in \mathcal{U}; ||\Delta\mathbf{g}_E|| \le \epsilon_E; ||\Delta\mathbf{L}_d^{\mathrm{E}}|| \le \epsilon_E \forall d \in \mathcal{D}; ||\Delta\mathbf{h}_E|| \le \epsilon_E$, where $\epsilon_{[\cdot]}$ denotes the error bound. Given these uncertainties, the imperfect channels are situated in the bounded region [13] defined as $\mathbf{G}_u \in \mathcal{G} = \Big\{\tilde{\mathbf{G}}_u + \Delta\mathbf{G}_u : ||\Delta\mathbf{G}_u|| \le \epsilon_u\Big\}$; $\mathbf{g}_u \in \mathcal{P} = \Big\{\tilde{\mathbf{g}}_u + \Delta\mathbf{g}_u : ||\Delta\mathbf{g}_u|| \le \epsilon_u\Big\}$; $\mathbf{G}_{IA} \in \mathcal{F} = \Big\{\tilde{\mathbf{G}}_{IA} + \Delta\mathbf{G}_{IA} : ||\Delta\mathbf{G}_{IA}|| \le \epsilon_u\Big\}$; $\mathbf{H}_d \in \mathcal{H} = \Big\{\tilde{\mathbf{H}}_d + \Delta\mathbf{H}_d : ||\Delta\mathbf{H}_d|| \le \epsilon_d\Big\}$; $\mathbf{h}_d \in \mathcal{S} = \Big\{\tilde{\mathbf{h}}_d + \Delta\mathbf{h}_d : ||\Delta\mathbf{h}_d|| \le \epsilon_d\Big\}$; $\mathbf{H}_{AI} \in \mathcal{T} = \Big\{\tilde{\mathbf{H}}_{AI} + \Delta\mathbf{H}_{AI} : ||\Delta\mathbf{H}_{AI}|| \le \epsilon_d\Big\}$; $\mathbf{b}_u^{\mathrm{E}} \in \mathcal{L} = \Big\{\tilde{\mathbf{b}}_u^{\mathrm{E}} + \Delta\mathbf{b}_u^{\mathrm{E}} : ||\Delta\mathbf{b}_u^{\mathrm{E}}|| \le \epsilon_E\Big\}$; $\mathbf{g}_E \in \mathcal{X} = \Big\{\tilde{\mathbf{g}}_E + \Delta\mathbf{g}_E : ||\Delta\mathbf{g}_E|| \le \epsilon_E\Big\}$; $\mathbf{L}_d^{\mathrm{E}} \in \mathcal{Y} = \Big\{\tilde{\mathbf{L}}_d^{\mathrm{E}} + \Delta\mathbf{L}_d^{\mathrm{E}} : ||\Delta\mathbf{L}_d^{\mathrm{E}}|| \le \epsilon_E\Big\}$; $\mathbf{h}_E \in \mathcal{Z} = \Big\{\tilde{\mathbf{h}}_E + \Delta\mathbf{h}_E : ||\Delta\mathbf{h}_E|| \le \epsilon_E\Big\}$.

III. Problem Formulation And Proposed Solution

In this study, our main objective is to optimize the total power by concurrently upholding a minimum performance level for B_u^{UL} and B_d^{DL}, all within the confines of available resource constraints and accounting for the iCSI at all nodes. Towards this, we formulate an optimization problem as

$$\textbf{(P1)} \min_{\mathbf{p},\mathbf{W},\mathbf{V},\boldsymbol{\theta},\boldsymbol{\phi}} \quad P^{\mathrm{Total}} \quad (10a)$$

$$\text{s.t.} \quad \sum\nolimits_{u=1}^{U} P_u||\mathbf{\Theta}\mathbf{g}_u||^2 + ||\mathbf{\Theta}||_F^2\sigma_I^2 \le P_I, \mathbf{g}_u \in \mathcal{P}, \quad (10b)$$

$$\sum\nolimits_{d=1}^{D} ||\mathbf{\Phi}\mathbf{H}_{AI}\mathbf{v}_d||^2 + ||\mathbf{\Phi}||_F^2\sigma_I^2 \le P_I, \mathbf{H}_{AI} \in \mathcal{A}, \quad (10c)$$

$$P_u \le P_{max}^u, \forall u, \quad (10d)$$

$$\sum\nolimits_{d=1}^{D} ||\mathbf{v}_d||^2 \le P_{max}^d, \quad (10e)$$

$$\eta_i \le \eta_{i,max}, i = \{1,2,...,K\}, \quad (10f)$$

$$\eta_r \le \eta_{r,max}, r = \{1,2,...,N\}, \quad (10g)$$

$$R_u^A \ge R_{min}^A, \mathbf{G}_u \in \mathcal{G}, \mathbf{g}_u \in \mathcal{P}, \mathbf{G}_{IA} \in \mathcal{F}, \forall u, \quad (10h)$$

$$R_d^D \ge R_{min}^D, \mathbf{H}_d \in \mathcal{H}, \mathbf{h}_d \in \mathcal{S}, \mathbf{H}_{AI} \in \mathcal{A}, \forall d, \quad (10i)$$

$$R^{sec} \ge R_{min}^{sec}, \quad (10j)$$

$$||\mathbf{w}_u|| = 1, \forall u, \quad (10k)$$

where $P^{\mathrm{Total}} = \sum_{u=1}^{U} P_u||\mathbf{\Theta}\mathbf{g}_u||^2 + \sum_{d=1}^{D}||\mathbf{\Phi}\mathbf{H}_{AI}\mathbf{v}_d||^2$, $\mathbf{p} = [P_1, \cdots, P_U]$, and $\mathbf{V} = [\mathbf{v}_1, \cdots, \mathbf{v}_D]$. Note that (10b) and (10c) represent the maximum amplification allowed at the ARIS1 and ARIS2, respectively, (10d) corresponds to the maximum transmit power available at B_u^{UL}, and (10e) corresponds to the maximum transmit power available at Alice. $\eta_{i,max}$ and $\eta_{r,max}$ are the maximum amplification coefficient. Constraint (10h) ensure a minimum rate of R_{min}^{A} at Alice, (10i) ensures a minimum rate of R_{min}^{D} at B_d^{DL}, and (10j) ensure a minimum secrecy rate. (10k) is the unit energy constraint corresponding to the decoding vector for each B_u^{UL}. Due to coupling of variables in (10a), (10b), (10c), (10h), (10i), and (10j), the problem (**P1**) is non-convex in nature. Therefore, in what follows, we adopt the AO technique to obtain optimum $\mathbf{p}$, $\mathbf{W}$, $\mathbf{V}$, $\mathbf{\Theta}$, and $\mathbf{\Phi}$. To further address this non-convex problem, we introduce auxiliary variables $\boldsymbol{\upsilon}^{\mathrm{A}}$, $\boldsymbol{\upsilon}^{\mathrm{D}}$, $\boldsymbol{\upsilon}^{\mathrm{AE}}$ and $\boldsymbol{\upsilon}^{\mathrm{DE}}$. Thus, (**P1**) is transformed as

$$\textbf{(P2)} \min_{\substack{\mathbf{p},\mathbf{W},\mathbf{V},\boldsymbol{\theta},\boldsymbol{\phi},\\ \boldsymbol{\upsilon}^{\mathrm{A}},\boldsymbol{\upsilon}^{\mathrm{D}},\boldsymbol{\upsilon}^{\mathrm{AE}},\boldsymbol{\upsilon}^{\mathrm{DE}}}} \quad P^{\mathrm{Total}} \quad (11a)$$

$$\text{s.t.} \quad R_u^{\mathrm{A}} \ge \upsilon_u^{\mathrm{A}}, \mathbf{G}_u \in \mathcal{G}, \mathbf{g}_u \in \mathcal{P}, \mathbf{G}_{IA} \in \mathcal{F}, \forall u, \quad (11b)$$

$$R_d^{\mathrm{D}} \ge \upsilon_d^{\mathrm{D}}, \mathbf{H}_d \in \mathcal{H}, \mathbf{h}_d \in \mathcal{S}, \mathbf{H}_{AI} \in \mathcal{A}, \forall d, \quad (11c)$$

$$R_u^{\mathrm{E}} \le \upsilon_u^{\mathrm{AE}}, \mathbf{b}_u^{\mathrm{E}} \in \mathcal{L}, \mathbf{g}_u \in \mathcal{P}, \mathbf{g}_E \in \mathcal{X}, \quad (11d)$$

$$R_d^{\mathrm{E}} \le \upsilon_d^{\mathrm{DE}}, \mathbf{L}_d^{\mathrm{E}} \in \mathcal{Y}, \mathbf{H}_{AI} \in \mathcal{A}, \mathbf{h}_E \in \mathcal{Z}, \quad (11e)$$

$$\upsilon_u^{\mathrm{A}} \ge R_{u,min}^{\mathrm{A}}, \forall u, \quad (11f)$$

$$\upsilon_d^{\mathrm{D}} \ge R_{d,min}^{\mathrm{D}}, \forall d, \quad (11g)$$

$$\sum_{u=1}^{U}(\upsilon_u^{\mathrm{A}} - \upsilon_u^{\mathrm{AE}}) + \sum_{d=1}^{\mathrm{D}}(\upsilon_d^{\mathrm{D}} - \upsilon_d^{\mathrm{DE}}) \ge R_{min}^{sec}, \quad (11h)$$

$$(10b) \sim (10g),$$

where $\boldsymbol{\upsilon}^{\mathrm{A}} = [\upsilon_1^{\mathrm{A}}, \cdots, \upsilon_U^{\mathrm{A}}]$, $\boldsymbol{\upsilon}^{\mathrm{D}}$=$[\upsilon_1^{\mathrm{D}}, \cdots, \upsilon_D^{\mathrm{D}}]$, $\boldsymbol{\upsilon}^{\mathrm{AE}}$= $[\upsilon_1^{\mathrm{AE}}, \cdots, \upsilon_U^{\mathrm{AE}}]$, and $\boldsymbol{\upsilon}^{\mathrm{DE}} = [\upsilon_1^{\mathrm{DE}}, \cdots, \upsilon_D^{\mathrm{DE}}]$. For the AO-based approach, $\mathbf{p}$, $\mathbf{W}$, $\mathbf{V}$, $\mathbf{\Theta}$ and $\mathbf{\Phi}$ are optimized alternatively, one-by-one, in an iterative manner, which is discussed in the next sub-sections.

A. Joint Optimization for $\mathbf{p}$, $\mathbf{W}$, and $\mathbf{V}$

For given $\mathbf{\Theta}$,$\mathbf{\Phi}$ the problem **(P2)** is reformulated to obtain sub-optimum $\mathbf{p}$, $\mathbf{W}$ and $\mathbf{V}$ as

$$\textbf{(P3)} \min_{\substack{\mathbf{p},\mathbf{W},\mathbf{V},\boldsymbol{\upsilon}^{\mathrm{A}},\\ \boldsymbol{\upsilon}^{\mathrm{D}},\boldsymbol{\beta},\boldsymbol{\xi},\boldsymbol{\delta}^{\mathrm{A}},\boldsymbol{\delta}^{\mathrm{D}},\boldsymbol{\varsigma}^{\mathrm{DL}}}} \quad P^{\mathrm{Total}} \quad (12a)$$

$$\text{s.t.} \quad P_u|\mathbf{w}_u^H(\mathbf{G}_u\boldsymbol{\theta})|^2 \ge (2^{\upsilon_u^{\mathrm{A}}} - 1)\beta_u^{\mathrm{A}}, \mathbf{G}_u \in \mathcal{G}, \forall u, \quad (12b)$$

$$\sum\nolimits_{i=1,i\neq u}^{U} \xi_{u,i}^{\mathrm{A}} + \delta_u^{\mathrm{A}} + P_u^{\mathrm{SI}} + ||\mathbf{w}_u||^2\sigma_1^2 \le \beta_u, \forall u, \quad (12c)$$

$$|\mathbf{w}_u^H(\mathbf{G}_i\boldsymbol{\theta})|^2 \le \frac{\xi_{u,i}^{\mathrm{A}}}{P_i}, \mathbf{G}_i \in \mathcal{G}, \forall u, i, \quad (12d)$$

$$||\mathbf{w}_u^H\mathbf{G}_{IA}\mathbf{\Theta}||^2 \le \frac{\delta_u^{\mathrm{A}}}{\sigma_I^2}, \mathbf{G}_{IA} \in \mathcal{F}, \quad (12e)$$

$$|(\boldsymbol{\phi}^H\mathbf{H}_d)\mathbf{v}_d|^2 \ge (2^{\upsilon_d^{\mathrm{D}}} - 1)\beta_d^{\mathrm{D}}, \mathbf{H}_d \in \mathcal{H}, \forall d. \quad (12f)$$

$$\sum\nolimits_{i=1,i\neq d}^{\mathrm{D}} \xi_{d,i}^{\mathrm{D}} + \delta_d^{\mathrm{D}} + P_d^{\mathrm{CCI}} + \sigma_d^2 \le \beta_d^{\mathrm{D}}, \forall d, \quad (12g)$$

$$|(\boldsymbol{\phi}^H\mathbf{H}_d)\mathbf{v}_i|^2 \le \xi_{d,i}^{\mathrm{D}}, \mathbf{H}_d \in \mathcal{H}, \forall d, i, \quad (12h)$$

$$||\mathbf{h}_d\mathbf{\Phi}||^2 \leq \frac{\delta_d^{\mathrm{D}}}{\sigma_I^2}, \mathbf{h}_d \in \mathcal{S}, \forall d, \tag{12i}$$

$$|(\boldsymbol{\phi}^H \mathbf{L}_d^{\mathrm{E}})\mathbf{v}_d|^2 \leq (2^{\upsilon_d^{\mathrm{DE}}}-1)\beta_d^{\mathrm{DE}}, \mathbf{L}_d^{\mathrm{E}} \in \mathcal{Y}, \tag{12j}$$

$$\sum_{i=1,i\neq d}^{\mathrm{D}} \varsigma_{d,i}^{\mathrm{DL}} + ||\mathbf{h}_E\mathbf{\Phi}||^2\sigma_I^2 + \epsilon_E^2||\mathbf{\Phi}||^2\sigma_I^2 + \sum_{u=1}^{U} P_u(|\mathbf{b}_u^{\mathrm{E},H}\boldsymbol{\theta}|^2 + \epsilon_E|\boldsymbol{\theta}|^2) + ||\mathbf{g}_E\mathbf{\Theta}||^2\sigma_I^2 + \epsilon_E^2||\mathbf{\Theta}||^2\sigma_I^2 + \sigma_E^2 \geq \beta_d^{\mathrm{DE}}, \tag{12k}$$

$$|(\boldsymbol{\phi}^H \mathbf{L}_d^{\mathrm{E}})\mathbf{v}_i|^2 \geq \varsigma_{d,i}^{\mathrm{DL}}, \mathbf{L}_d^{\mathrm{E}} \in \mathcal{Y}, \forall d, i, \tag{12l}$$

$$P_u|\mathbf{b}_u^{\mathrm{E},H}\boldsymbol{\theta}|^2 \leq (2^{\upsilon_u^{\mathrm{AE}}}-1)\beta_u^{\mathrm{AE}}, \mathbf{b}_u^{\mathrm{E}} \in \mathcal{L}, \tag{12m}$$

$$\sum_{i=1,i\neq u}^{U} P_i|\mathbf{b}_i^{\mathrm{E},H}\boldsymbol{\theta}|^2 + ||\mathbf{g}_E\mathbf{\Theta}||^2\sigma_I^2 + \sigma_E^2 + \sum_{d=1}^{\mathrm{D}} \varsigma_{d,d}^{\mathrm{DL}} + ||\mathbf{h}_E\mathbf{\Phi}||^2\sigma_I^2 + \geq \beta_u^{\mathrm{AE}}, \tag{12n}$$

$$(10\mathrm{d}), (10\mathrm{e}), (11\mathrm{f}) \sim (11\mathrm{h}),$$

where $\boldsymbol{\beta}^A$=$[\beta_1^A, \cdots, \beta_U^A]$, $\boldsymbol{\beta}^D$=$[\beta_1^D, \cdots, \beta_U^D]$, $\boldsymbol{\beta}^{\mathrm{AE}}$=$[\beta_1^{\mathrm{AE}}, \cdots, \beta_U^{\mathrm{AE}}]$, $\boldsymbol{\beta}^{\mathrm{DE}}$=$[\beta_1^{\mathrm{DE}}, \cdots, \beta_D^{\mathrm{DE}}]$, $\boldsymbol{\beta}$=$\{\boldsymbol{\beta}^A, \boldsymbol{\beta}^D, \boldsymbol{\beta}^{\mathrm{AE}}, \boldsymbol{\beta}^{\mathrm{DE}}\}$, $\boldsymbol{\xi}^A$=$[\xi_1^A, \cdots, \xi_U^A]$, $\boldsymbol{\xi}^D$=$[\xi_1^D, \cdots, \xi_D^D]$, $\boldsymbol{\xi}^{\mathrm{AE}}$=$[\xi_1^{\mathrm{AE}}, \cdots, \xi_U^{\mathrm{AE}}]$, $\boldsymbol{\xi}^{\mathrm{DE}}$=$[\xi_1^{\mathrm{DE}}, \cdots, \xi_D^{\mathrm{DE}}]$, $\boldsymbol{\xi}$=$\{\boldsymbol{\xi}^A, \boldsymbol{\xi}^D, \boldsymbol{\xi}^{\mathrm{AE}}, \boldsymbol{\xi}^{\mathrm{DE}}\}$, $\boldsymbol{\delta}^A$=$[\delta_1^A, \cdots, \delta_U^A]$, and $\boldsymbol{\delta}^D$=$[\delta_1^D, \cdots, \delta_D^D]$.The optimization problem **(P3)** is non-convex due to the worst-case quadratic inequality constraints. Using the linear-matrix inequality (LMI) and second-order cone (SOC) constraints, we convexify the problem into a tractable problem using the following Lemmas.

Lemma 1. *The closed form of* $|(\tilde{\mathbf{h}} + \Delta\mathbf{h})^H\mathbf{w}|$ *is given by*

$$\xi^* = |\tilde{\mathbf{h}}^H\mathbf{w}| + \epsilon||\mathbf{w}||_2. \tag{13}$$

Lemma 2. *If* $\Delta\mathbf{G}_u$ *is bounded by* $||\Delta\mathbf{G}_u|| = \epsilon$*, i.e.,* $\|vec(\Delta\mathbf{G}_u)\|_2 \leq \epsilon_u$*, then its upper bound is given as*

$$||\mathbf{w}^H\Delta\mathbf{G}_u\mathbf{\Theta}|| \leq \epsilon||\mathbf{\Theta}^T \otimes \mathbf{w}^H||. \tag{14}$$

Proof. For the proof, refer to the **Lemma 1** and **Lemma 2** in [16]. ■

Using **Lemma 1**, **Lemma 2** and the Taylor's approximation at $\xi_{u,i}^{\mathrm{A},(n)}$ and $P_i^{(n)}$, (12d) can be equivalently written as

$$|\mathbf{w}_u^H(\tilde{\mathbf{G}}_i\boldsymbol{\theta})| + \epsilon_u||\mathbf{w}_u \otimes \boldsymbol{\theta}||_2 \leq \sqrt{\frac{\xi_{u,i}^{\mathrm{A},(n)}}{P_i^{(n)}}} + \frac{\xi_{u,i}}{2}\sqrt{\frac{P_i^{(n)}}{\xi_{u,i}^{\mathrm{A},(n)}}} - \sqrt{\frac{\xi_{u,i}^{\mathrm{A},(n)}P_i^{(n)}}{2}} - \frac{P_i}{2}\sqrt{\frac{1}{\xi_{u,i}^{\mathrm{A},(n)}(P_i^{(n)})^3}} + \frac{1}{2}\sqrt{\frac{1}{\xi_{u,i}^{\mathrm{A},(n)}P_i^{(n)}}}. \tag{15}$$

Similarly constraints (12e), (12h), (12i), (12j), (12m), and (12n) are transformed as

$$||\mathbf{w}_u^H\tilde{\mathbf{G}}_{IA}\mathbf{\Theta}||_2 + \epsilon_u||\mathbf{\Theta} \otimes \mathbf{w}_u^H||_2 \leq \frac{\sqrt{\delta_u^{\mathrm{A},(n)}}}{2\sigma_I} + \frac{\delta_u}{2\sigma_I\sqrt{\delta_u^{\mathrm{A},(n)}}}, \tag{16}$$

$$|(\boldsymbol{\phi}^H\tilde{\mathbf{H}}_d)\mathbf{v}_i| + \epsilon_d||\mathbf{v}_i \otimes \boldsymbol{\phi}||_2 \leq \frac{\sqrt{\xi_{d,i}^{\mathrm{D},(n)}}}{2} + \frac{\xi_{d,i}^{\mathrm{D}}}{2\sqrt{\xi_{d,i}^{\mathrm{D},(n)}}}, \tag{17}$$

$$||\tilde{\mathbf{h}}_d\mathbf{\Phi}||_2 + \epsilon_u||\mathbf{\Phi}||_2 \leq \frac{\sqrt{\delta_d^{\mathrm{D},(n)}}}{2\sigma_I} + \frac{\delta_d^{\mathrm{D}}}{2\sigma_I\sqrt{\delta_d^{\mathrm{D},(n)}}}, \tag{18}$$

$$|(\boldsymbol{\phi}^H\tilde{\mathbf{L}}_d^{\mathrm{E}})\mathbf{v}_d| + \epsilon_E||\mathbf{v}_d \otimes \boldsymbol{\phi}||_2 \leq \sqrt{(2^{\upsilon_d^{\mathrm{DE},(n)}}-1)\beta_d^{\mathrm{DE},(n)}} + \frac{\beta_d^{\mathrm{DE,(n)}}\ln(2)\cdot 2^{\upsilon_d^{\mathrm{DE},(n)}}}{2\sqrt{(2^{\upsilon_d^{\mathrm{DE},(n)}}-1)\beta_d^{\mathrm{DE},(n)}}}(\upsilon_d^{\mathrm{DE}} - \upsilon_d^{\mathrm{DE},(n)}) + \frac{2^{\upsilon_d^{\mathrm{DE},(n)}}-1}{2\sqrt{(2^{\upsilon_d^{\mathrm{DE},(n)}}-1)\beta_d^{\mathrm{DE},(n)}}}(\beta_d^{\mathrm{DE}} - \beta_d^{\mathrm{DE},(n)}), \tag{19}$$

$$|\tilde{\mathbf{b}}_u^{\mathrm{E},H}\boldsymbol{\theta}| + \epsilon_E||\boldsymbol{\theta}||_2 \leq f(\upsilon_u^{\mathrm{AE}}, \beta_u^{\mathrm{AE}}, P_u), \tag{20}$$

$$\sum_{i=1,i\neq u}^{U} P_i(|\tilde{\mathbf{b}}_i^{\mathrm{E},H}\boldsymbol{\theta}|^2 + \epsilon_E|\boldsymbol{\theta}|^2) + ||\tilde{\mathbf{g}}_E\mathbf{\Theta}||^2\sigma_I^2 + \sigma_E^2 + \epsilon_E^2 ||\mathbf{\Theta}||^2\sigma_I^2 + \sum_{d=1}^{\mathrm{D}} \varsigma_{d,d}^{\mathrm{DL}} + ||\mathbf{h}_E\mathbf{\Phi}||^2\sigma_I^2 + \epsilon_E^2||\mathbf{\Phi}||^2\sigma_I^2 \geq \beta_u^{\mathrm{AE}}, \tag{21}$$

where

$$f(\upsilon_u^{\mathrm{AE}}, \beta_u^{\mathrm{AE}}, P_u) = \sqrt{\frac{(2^{\upsilon_u^{\mathrm{AE},(n)}}-1)\beta_u^{\mathrm{AE},(n)}}{P_u^{(n)}}} + \frac{\ln 2 \cdot 2^{\upsilon_u^{\mathrm{AE},(n)}}\beta_u^{\mathrm{AE},(n)}}{2\sqrt{P_u^{(n)}(2^{\upsilon_u^{\mathrm{AE},(n)}}-1)\beta_u^{\mathrm{AE},(n)}}}(\upsilon_u^{\mathrm{AE}} - \upsilon_u^{\mathrm{AE},(n)}) + \frac{2^{\upsilon_u^{\mathrm{AE},(n)}}-1}{2\sqrt{P_u^{(n)}(2^{\upsilon_u^{\mathrm{AE},(n)}}-1)\beta_u^{\mathrm{AE},(n)}}}(\beta_u^{\mathrm{AE}} - \beta_u^{\mathrm{AE},(n)}) - \frac{(2^{\upsilon_u^{\mathrm{AE},(n)}}-1)\beta_u^{\mathrm{AE},(n)}}{2(P_u^{(n)})^2\sqrt{P_u^{(n)}(2^{\upsilon_u^{\mathrm{AE},(n)}}-1)\beta_u^{\mathrm{AE},(n)}}}(P_u - P_u^{(n)}). \tag{22}$$

To address the constraints (12b), (12f), and (12k), the following Lemmas are introduced. At $\mathbf{w}_u^{(n)}$, $\boldsymbol{\theta}^{(n)}$, $P_u^{(n)}$, $\upsilon_u^{A(n)}$, and $\beta_u^{A(n)}$ the constraint transformed with imperfections of $\mathbf{G}_u$ as

$$\mathrm{vec}^T(\Delta\mathbf{G}_u)\mathbf{F}_u\mathrm{vec}(\Delta\mathbf{G}_u^* + 2Re\{\mathbf{f}_u^T\mathrm{vec}(\Delta\mathbf{G}_u^*)\} + f_u - \lambda_u^A \geq 0, \mathbf{G}_u \in \mathcal{G}, \forall u, \mathcal{U} \tag{23}$$

where $\mathbf{F}_u$= $\mathbf{w}_u^{(n)}\mathbf{w}_u^{(n),H} \otimes \boldsymbol{\theta}^*\boldsymbol{\theta}^{(n),T} + \mathbf{w}_u^{(n)}\mathbf{w}_u^{(n),H} \otimes \boldsymbol{\theta}^{(n),*}\boldsymbol{\theta}^{(n),T} - \mathbf{w}_u^{(n)}\mathbf{w}_u^{(n),H} \otimes \boldsymbol{\theta}^{(n),*}\boldsymbol{\theta}^{(n),T}$, $\mathbf{f}_u$ = $\mathrm{vec}(\mathbf{w}_u^{(n)}\mathbf{w}_u^{(n),H}(\tilde{\mathbf{G}}_u\boldsymbol{\theta})\boldsymbol{\theta}^{(n),H}) + \mathrm{vec}(\mathbf{w}_u^{(n)}\mathbf{w}_u^{(n),H}(\tilde{\mathbf{G}}_u\boldsymbol{\theta}^{(n)})\boldsymbol{\theta}^H) - \mathrm{vec}(\mathbf{w}_u^{(n)}\mathbf{w}_u^{(n),H}(\tilde{\mathbf{G}}_u\boldsymbol{\theta}^{(n)})\boldsymbol{\theta}^{(n),H})$, f_u = $2Re\big\{((\mathbf{w}_u^{(n),H}\tilde{\mathbf{G}}_u)\boldsymbol{\theta}\boldsymbol{\theta}^{(n),H}(\tilde{\mathbf{G}}_u\mathbf{w}_u^{(n)}))\big\} - \big((\mathbf{w}_u^{(n),H}\tilde{\mathbf{G}}_u)\boldsymbol{\theta}^{(n)}\boldsymbol{\theta}^H(\tilde{\mathbf{G}}_u\mathbf{w}_u^{(n)})\big)$, λ_u^A= $\frac{\beta_u^A\upsilon_u^{A(n)}}{P_u^{(n)}} + \frac{\beta_u^{A(n)}\upsilon_u^A}{P_u^{(n)}} - \frac{\beta_u^{A(n)}\upsilon_u^{A(n)}P_u}{(P_u^{(n)})^2} - \frac{2\beta_u^{A(n)}\upsilon_u^{A(n)}}{P_u^{(n)}}$. Further, we simplify (23) using S-procedure [12], which is shown in the following lemma. Using [12, Lemma 1], (23) is transformed as the following LMI constraint

$$\begin{bmatrix} \mathbf{F}_u + \mu_u\mathbf{I} & \mathbf{f}_u \\ \mathbf{f}_u & c_u \end{bmatrix} \geq \mathbf{0}, \mu_u \geq 0, \forall u, \tag{24}$$

where $\boldsymbol{\mu} = [\mu_1, \cdots, \mu_U] \geq 0$ is the added slack variable and $c_u = f_u - \lambda_u^A - \mu_u\epsilon^2$. At $\mathbf{v}_d^{(n)}$, $\boldsymbol{\phi}^{(n)}$, $\upsilon_d^{D(n)}$, and $\beta_d^{D,(n)}$ the constraint transformed with imperfection of $\mathbf{H}_d$ as

$$\mathrm{vec}^T(\Delta\mathbf{H}_d)\mathbf{Y}_d\mathrm{vec}(\Delta\mathbf{H}_d^* + 2Re\{\mathbf{y}_d^T\mathrm{vec}(\Delta\mathbf{H}_d^*)\} + y_d \geq \beta_d^D\gamma_d, \mathbf{H}_d \in \mathcal{H}, \forall d \in \mathcal{D}, \tag{25}$$

where $\mathbf{Y}_d = \mathbf{v}_d \mathbf{v}_d^{(n),H} \otimes \boldsymbol{\phi}^* \boldsymbol{\phi}^{(n),T} + \mathbf{v}_d^{(n)} \mathbf{v}_d^H \otimes \boldsymbol{\phi}^{(n),*} \boldsymbol{\phi}^T - (\mathbf{v}_d^{(n)} \mathbf{v}_d^{(n),H} \otimes \boldsymbol{\phi}^{(n),*} \boldsymbol{\phi}^{(n),T})$, $\mathbf{y}_d = \text{vec}\big(\boldsymbol{\phi}(\boldsymbol{\phi}^{(n),H} \tilde{\mathbf{H}}_d) \mathbf{v}_d^{(n)} \mathbf{v}_d^H\big) + \text{vec}\big(\boldsymbol{\phi}^{(n)} \big(\boldsymbol{\phi}^H \tilde{\mathbf{H}}_d\big) \mathbf{v}_d \mathbf{v}_d^{(n),H}\big) - \text{vec}\big(\boldsymbol{\phi}^{(n)} (\boldsymbol{\phi}^{(n),H} \tilde{\mathbf{H}}_d) \mathbf{v}_d^{(n)} \mathbf{v}_d^{(n),H}\big)$, $y_d = 2Re\big\{\big((\boldsymbol{\phi}^{(n),H} \tilde{\mathbf{H}}_d) \mathbf{v}_d^{(n)} \mathbf{v}_d^H (\tilde{\mathbf{H}}_d^H \boldsymbol{\phi})\big)\big\} - \big((\boldsymbol{\phi}^{(n),H} \tilde{\mathbf{H}}_d) \mathbf{v}_d^{(n)} \mathbf{v}_d^{(n),H} (\tilde{\mathbf{H}}_d^H \boldsymbol{\phi}^{(n)})\big)$, $\gamma_d = 2^{\upsilon_d^D} - 1$.
The corresponding LMI for the constraint (12f) with bounded CSI error is obtained by using [12, Lemma 1] and (25)

$$\begin{bmatrix} \mathbf{Y}_d + \varpi_d \mathbf{I} & \mathbf{y}_d \\ \mathbf{y}_d & c_d \end{bmatrix} \geq \mathbf{0}, \forall d, \tag{26}$$

where $\boldsymbol{\varpi} = [\varpi_1, \cdots, \varpi_D] \geq 0$ represented the slack variable and $c_d = y_d - \lambda_d^D - \varpi_d \epsilon_d^2$ and $\lambda_d^D = \beta_d \gamma_d$. Substituting $\mathbf{L}_d^{\text{E}} = \tilde{\mathbf{L}}_d^{\text{E}} + \Delta \mathbf{L}_d^{\text{E}}$ into (12l) and after some manipulation, we obtain

$$\begin{aligned} \text{vec}^T(\Delta \mathbf{L}_i^{\text{E}}) \mathbf{E}_{d,i}^{\text{D}} \text{vec}(\Delta \mathbf{L}_i^{\text{E},*}) + 2Re\{\mathbf{e}_{d,i}^{D,T} \text{vec}(\Delta \mathbf{L}_i^{\text{E},*})\} \\ + e_{d,i}^{\text{D}} \geq \varsigma_{d,i}^{\text{DL}}, \mathbf{L}_d^{\text{E}} \in \mathcal{Y}, \mathbf{h}_E \in \mathcal{Z}, \end{aligned} \tag{27}$$

where $\mathbf{E}_{d,i}^{\text{D}} = \mathbf{v}_i \mathbf{v}_i^{(n),H} \otimes \boldsymbol{\phi}^* \boldsymbol{\phi}^{(n),T} + \mathbf{v}_i^{(n)} \mathbf{v}_i^H \otimes \boldsymbol{\phi}^{(n),*} \boldsymbol{\phi}^T - (\mathbf{v}_i^{(n)} \mathbf{v}_i^{(n),H} \otimes \boldsymbol{\phi}^{(n),*} \boldsymbol{\phi}^{(n),T})$, $\mathbf{e}_{d,i}^{\text{D}} = \text{vec}(\boldsymbol{\phi}(\tilde{\mathbf{L}}_{d,i}^{\text{E}} \boldsymbol{\phi}^{(n),H}) \mathbf{v}_i^{(n)} \mathbf{v}_i^H) + \text{vec}(\boldsymbol{\phi}^{(n)} (\tilde{\mathbf{L}}_{d,i}^{\text{E}} \boldsymbol{\phi}^H) \mathbf{v}_i \mathbf{v}_i^{(n),H}) - \text{vec}(\boldsymbol{\phi}^{(n)} (\tilde{\mathbf{L}}_{d,i}^{\text{E}} \boldsymbol{\phi}^{(n),H}) \mathbf{v}_i^{(n)} \mathbf{v}_i^{(n),H})$, $e_{d,i}^{\text{D}} = 2Re\{((\tilde{\mathbf{L}}_{d,i}^{\text{E}} \boldsymbol{\phi}^{(n),H}) \mathbf{v}_i^{(n)} \mathbf{v}_i^H (\tilde{\mathbf{L}}_{d,i}^{\text{E},H} \boldsymbol{\phi}))\} - ((\tilde{\mathbf{L}}_{d,i}^{\text{E}} \boldsymbol{\phi}^{(n),H}) \mathbf{v}_i^{(n)} \mathbf{v}_i^{(n),H} (\tilde{\mathbf{L}}_{d,i}^{\text{E},H} \boldsymbol{\phi}^{(n)}))$. Using [12, Lemma 1], the equivalent LMI for the constraint (12l) with bounded CSI error is written as

$$\begin{bmatrix} \mathbf{E}_{d,i}^{\text{D}} + \tau_d \mathbf{I} & \mathbf{e}_{d,i}^{\text{D}} \\ \mathbf{e}_{d,i}^{D,H} & c_{d,i}^{\text{DE}} \end{bmatrix} \geq \mathbf{0}, \tag{28}$$

where $\boldsymbol{\tau} = [\tau_1, \cdots, \tau_D] \geq 0$ is the slack variable and $c_{d,i}^{\text{DE}} = e_{d,i}^{\text{D}} - \varsigma_{d,i}^{\text{DL}} - \tau_d \epsilon_E^2$. Finally, using the above LMIs and SOC constraints from (15), (16), (17), (18), (20), (19), (24), (26) and (28), the problem (**P3**) can be simplified as

$$\begin{aligned} \textbf{(P4)} \quad & \min_{\substack{\mathbf{p}, \mathbf{W}, \mathbf{V}, \boldsymbol{\upsilon}^{\text{A}}, \\ \boldsymbol{\upsilon}^{\text{D}}, \boldsymbol{\beta}, \boldsymbol{\xi}, \boldsymbol{\delta}^{\text{A}}, \boldsymbol{\delta}^{\text{D}}, \boldsymbol{\varsigma}^{\text{DL}}}} \quad P^{\text{Total}} \\ & \text{s.t.} \quad (10\text{d}), (10\text{e}), (11\text{f}) \sim (11\text{h}), \\ & \qquad (15) \sim (19), (24), (26), (28). \end{aligned} \tag{29}$$

It can be noted that the simplified problem **(P4)** is a standard convex problem [17], and thus, CVX can be used to solve it.

B. ARIS Beamforming Design

In this subsection, the optimal ARIS beamformer $\boldsymbol{\Theta}$ and $\boldsymbol{\Phi}$ are designed for given $\mathbf{p}$ and $\mathbf{V}$. In such case, the optimization problem can be expressed as

$$\begin{aligned} \textbf{(P5)} \quad & \min_{\boldsymbol{\theta}, \boldsymbol{\phi}, \boldsymbol{\upsilon}^A, \boldsymbol{\upsilon}^D, \boldsymbol{\beta}, \boldsymbol{\xi}, \boldsymbol{\delta}^A, \boldsymbol{\delta}^D} \quad P^{\text{Total}} \\ & \text{s.t.} \quad (10\text{b}), (10\text{c}), (10\text{f}), (10\text{g}), (11\text{f}) \sim (11\text{h}), \\ & \qquad (15) \sim (19), (24), (26), (28). \end{aligned} \tag{30}$$

It is noteworthy that the constraints outlined in the problem **(P5)** are convex. Thus, it is solved by adopting CVX [17]. Finally, using the aforementioned discussions, we propose an AO-based algorithm, **Algorithm 1**, which solves the problem **(P1)** and jointly obtains optimum values of $\mathbf{p}$, $\mathbf{W}$, $\mathbf{V}$, $\boldsymbol{\Theta}$, and $\boldsymbol{\Phi}$. Each iteration solves problem **(P4)** and problem **(P5)** using CVX to obtain $\mathbf{p}$ and $\mathbf{V}$ (step 3), $\boldsymbol{\Theta}$ and $\boldsymbol{\Phi}$ (step 4), respectively. This process continues repeatedly till convergence is achieved.

Algorithm 1 Proposed Algorithm for Joint Optimization

Initialize $n = 1$
Repeat:
Initialize $n = 0$, $P_u^{(0)}$, $\mathbf{W}^{(0)}$, $\mathbf{V}^{(0)}$, $\boldsymbol{\Theta}^{(0)}$, $\boldsymbol{\Phi}^{(0)}$
Optimize $\mathbf{p}$, $\mathbf{W}$, and $\mathbf{V}$ given $\boldsymbol{\Theta}$, and $\boldsymbol{\Phi}$ using CVX (**P4**).
Optimize $\boldsymbol{\Theta}$ and $\boldsymbol{\Phi}$ given $\mathbf{p}^{(n+1)}$, $\mathbf{W}^{(n+1)}$, and $\mathbf{V}^{(n+1)}$ using CVX (**P5**).
$n = n + 1$,
Until: Convergence
Output $(\mathbf{p}, \mathbf{W}, \mathbf{V}, \boldsymbol{\Theta}, \boldsymbol{\Phi})$

Further, the complexity of **Algorithm 1** mainly depends on the computation of LMIs in steps 3 and 4. Consequently, from [12], the approximate computational complexity of step 3 is given by $C_1 = \mathcal{O}\Big([\big(2(KM_r+1)+2(NM_t+1)+K+M_r+1+N+M_t+1+2(K+1)+2(N+1)\big)]^{1/2} n_1 \Big(n_1^2 + n_1\big(2(KM_r+1)+2(NM_t+1)+KM_r+1+N+M_t+1+2(K+1)+(N+1)\big)^2 + \big(2(KM_r+1)+2(NM_t+1)+K+M_r+1+N+M_t+1+2(K+1)+2(N+1)\big)^3\Big)\Big)$ where $n_1 = UDM_rM_t$. Similarly, the approximate computational complexity of step 4 is $C_2 = \mathcal{O}\Big([\big(2(KM_r+1)+2(NM_t+1)+K+M_r+1+N+M_t+1+2(K+1)+2(N+1)\big)]^{1/2} n_1 \Big(n_1^2 + n_1\big(2(KM_r+1)+2(NM_t+1)+KM_r+1+N+M_t+1+2(K+1)+(N+1)\big)^2 + \big(2(KM_r+1)+2(NM_t+1)+K+M_r+1+N+M_t+1+2(K+1)+2(N+1)\big)^3\Big)\Big)$ where $n_2 = UDKN$. Thus, the total complexity of the proposed algorithm is given by $C_1 + C_2$.

IV. Numerical Example

In this section, numerous graphical results have been presented obtained using extensive numerical simulation to demonstrate the effectiveness and convergence of the suggested algorithms. We assume that Alice is positioned at (0, 0), Eve is located at (0, 30m), ARIS1 is positioned at (-10, 15), ARIS2 is located at (10, 15), users U = 3 and users D = 3 are scattered at (0, 0) accordingly, in a circle with a radius of R = 20m. This gives us a two-dimensional coordinate space for each node's location. Additionally, considering the line-of-sight (LoS) nature of the ARIS-aided links, all the channels are modeled following the Rician distribution [13]; however, details are omitted due to the paucity of the space. Unless stated otherwise, for the sake of simulations, $\mathcal{K}$ = 5, β = -30, $\eta_{i,max} = \eta_{r,max} = \eta_{max}$ = 10, and the exponential coefficient for large scale fading, denoted as α, is set to 2.1. The noise power levels are specified as $\sigma_1^2 = \sigma_d^2 = \sigma_I^2 = \sigma_E^2$ = -90dBm [15], $\epsilon_u = \epsilon_d = \epsilon_E = \epsilon$ = -10dBm. Each reflecting element has the same amplification factor, denoted as P_I, set to 10dBm unless otherwise instructed [7].

Fig. 2 depicts the convergence behaviour of the proposed algorithm. It can be observed that the solution provided by the proposed algorithm converges after a few iterations,

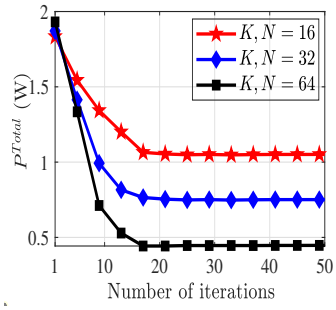

Fig. 2: Convergence.

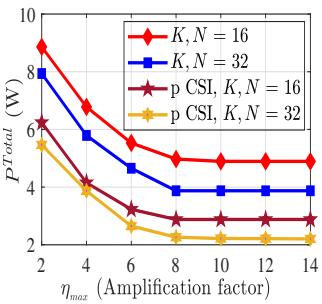

Fig. 3: P^{Total} vs η_{max}.

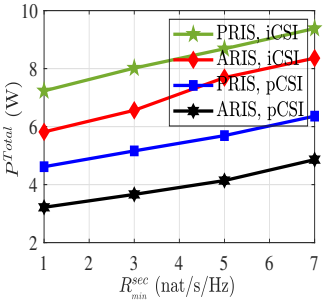

Fig. 4: P^{Total} vs R^{sec}_{min}.

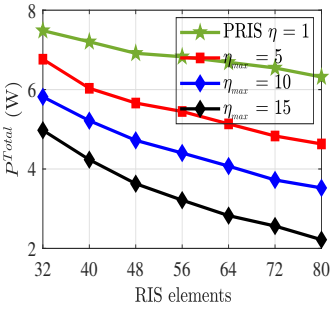

Fig. 5: P^{Total} vs RIS elements.

which validates its efficacy. Additionally, the P^{Total} consumption decreases with an increase in K and N. This is because of the rise in beamforming gain which leads in a significant boost in the received signal strength. Fig. 3 illustrates the behaviour of P^{Total} w.r.t. η_{max} for different values of K, N with M_r = 4, M_t = 4, P^u_{max} = 15dBm, P^d_{max} = 15dBm, and ϵ = -10dBm. It can be seen that the availability of larger η_{max} leads to significant decrease in the required P^{Total} to achieve desired QoS. The main reason for such behaviour is the fact that the higher amplification provides an extra freedom to lower the transmit power at the uplink users and Alice. Furthermore, compared to the pCSI, the performance decrease due to iCSI can also be seen, which is because of the net reduction in the SINR at each receiving node.

Fig. 4 shows the plot of P^{Total} versus R^{sec}_{min} obtained with K = 16, N = 16, M_r = 4, M_t = 4, P^u_{max} = 15dBm, P^d_{max} = 15dBm, and ϵ = -10dBm. As evident, P^{Total} rises proportionally with an increase in R^{sec}_{min}. This is because achieving a higher QoS at both uplink and downlink transmission demands more transmit power from each B^{UL}_u and Alice. It can also be seen that the use of multiple ARIS outperforms the conventional PRIS. This is because the PRIS suffers from "double fading" effect and hence requires larger power for achieving the same QoS. Fig. 5 depicts the plot of P^{Total} versus ARIS elements ($K = N$) for different η_{max} values with parameters M_r = 4, M_t = 4, $P^u_{max} = P^d_{max}$ = 15dBm, and ϵ = -10dBm. It can be observed that, as discussed in Fig. 5, with an increase in elements, there is a significant reduction in P^{Total} to achieve the desired QoS. Additionally, it can also be seen that compared to PRIS, the use of ARIS provides more greener communication.

V. Conclusion

In this paper, we investigated the performance of a multi-ARIS-aided secure FD network under the impact of norm-bounded iCSI. We formulated a power minimization problem that ensures the desired QoS within available resource constraints. We proposed an AO algorithm that provides robust and secure transmission design. The simulation results show that, depending on the constraints, the proper choice of amplification coefficient and phase shift designs avoids unnecessary power wastage at the ARIS leading to a greener, robust and secure communications.

References

[1] H. Tataria, M. Shafi, A. F. Molisch, M. Dohler, H. Sjöland, and F. Tufvesson, "6G wireless systems: Vision, requirements, challenges, insights, and opportunities," *Proc. IEEE*, vol. 109, no. 7, pp. 1166–1199, Jul. 2021.

[2] S. Han, J. Wang, L. Xiao, and C. Li, "Broadcast secrecy rate maximization in UAV-empowered IRS backscatter communications," *IEEE Tran. Wireless Commun.*, vol. 22, no. 10, pp. 6445–6458, Oct. 2023.

[3] A. Mukhopadhyay, K. Singh, F.-S. Tseng, S. K. Singh, K. Dev, and C. Pan, "A tutorial on near-field driven 6G networks," *IEEE Commun. Survs. Tuts.*, pp. 1–1, 2025.

[4] G. C. Alexandropoulos, K. D. Katsanos, M. Wen, and D. B. Da Costa, "Counteracting eavesdropper attacks through reconfigurable intelligent surfaces: A new threat model and secrecy rate optimization," *IEEE Open J. Commun. Soc.*, vol. 4, pp. 1285–1302, Jun. 2023.

[5] S. Pala, O. Taghizadeh, M. Katwe, K. Singh, C.-P. Li, and A. Schmeink, "Secure RIS-assisted hybrid beamforming design with low-resolution phase shifters," *IEEE Trans. Wireless Commun.*, pp. 1–1, 2024.

[6] S. Singh, A. Raviteja, K. Singh, S. K. Singh, A. Kaushik, and M.-L. Ku, "Secrecy rate maximization for active RIS-aided robust uplink NOMA communications," *IEEE Wireless Commun. Lett.*, vol. 13, no. 11, pp. 2960–2964, Nov 2024.

[7] R. Long, Y.-C. Liang, Y. Pei, and E. G. Larsson, "Active reconfigurable intelligent surface-aided wireless communications," *IEEE Trans. Wireless Commun.*, vol. 20, no. 8, pp. 4962–4975, Aug. 2021.

[8] J. Yaswanth, M. Katwe, K. Singh, S. Prakriya, and C. Pan, "Robust beamforming design for Active-RIS Aided MIMO SWIPT communication system: A power minimization approach," *IEEE Trans. Wireless Commun.*, vol. 23, no. 5, pp. 4767–4785, May 2024.

[9] Z. Zhang, L. Dai, X. Chen, C. Liu, F. Yang, R. Schober, and H. V. Poor, "Active RIS vs. passive RIS: Which will prevail in 6G?" *IEEE Trans. Commun.*, vol. 71, no. 3, pp. 1707–1725, Mar. 2023.

[10] L. Dong, H.-M. Wang, and J. Bai, "Active reconfigurable intelligent surface aided secure transmission," *IEEE Trans. Veh. Teclmol.*, vol. 71, no. 2, pp. 2181–2186, Feb. 2022.

[11] D. Xu, X. Yu, D. W. Kwan Ng, and R. Schober, "Resource allocation for active IRS-assisted multiuser communication systems," in *Proc. Asilomar Conf. Signals Syst. Computers*, Pacific Grove, CA, USA, Oct. 2021, pp. 113–119.

[12] G. Zhou *et al.*, "A framework of robust transmission design for IRS-aided MISO communications with imperfect cascaded channels," *IEEE Trans. Signal Process.*, vol. 68, pp. 5092–5106, 2020.

[13] R. Allu, O. Taghizadeh, S. K. Singh, K. Singh, and C.-P. Li, "Robust beamformer design in active RIS-assisted multiuser MIMO cognitive radio networks," *IEEE Trans. Cogn. Commun. Netw.*, vol. 9, no. 2, pp. 398–413, Apr. 2023.

[14] W. Lv, J. Bai, Q. Yan, and H. M. Wang, "RIS-assisted green secure communications: Active RIS or passive RIS?" *IEEE Wireless Commun. Lett.*, vol. 12, no. 2, pp. 237–241, Feb. 2023.

[15] L. Dong *et al.*, "Robust and secure transmission over active reconfigurable intelligent surface aided multi-user system," *IEEE Trans. Veh. Teclmol.*, vol. 72, no. 9, pp. 11 515–11 531, Sep. 2023.

[16] S. Chandrasekaran, G. Golub, M. Gu, and A. Sayed, "Parameter estimation in the presence of bounded modeling errors," *IEEE Signal Process. Lett.*, vol. 4, no. 7, pp. 195–197, Jul. 1997.

[17] S. P. Boyd and L. Vandenberghe, *Convex optimization*. Cambridge university press, 2004.